Hydrodynamics of a Gas-Liquid-Solid Fluidized Bed with Hollow Cylindrical Particles

Published in **Chemical Engineering and Processing: Process Intesification (2008)**

http://dx.doi.org/10.1016/j.cep.2008.04.003

Hydrodynamics of a Gas-Liquid-Solid Fluidized Bed with Hollow Cylindrical Particles

H. M. Jena[1*], G. K. Roy[1] and B. C. Meikap[2]

[1]*Department of Chemical Engineering, National Institute of Technology (NIT), Rourkela, Orissa, Pin - 769008, India*

[2]*Department of Chemical Engineering, Indian Institute of Technology (IIT), Kharagpur, P.O. Kharagpur Technology, West Bengal, Pin - 721302, India*

Corresponding author: H. M. Jena, Department of Chemical Engineering, National Institute of Technology (NIT), Rourkela-769008, INDIA, Telephone: 91-661-2462264(O) / 2463264(R), fax: +91-661-2462999, E-mail: hara.jena@gmail.com, hmjena@nitrkl.ac.in

Abstract

The hydrodynamic characteristics viz. the pressure drop, bed expansion and phase holdup profile of a co-current three-phase fluidized bed with an antenna type air sparger

have been determined. Correlations for minimum liquid fluidization velocity, bed voidage and gas holdup have been developed. The bed voidage is found to increase with the increase of both liquid and gas velocities. The gas holdup increases with gas Froude number, but decreases with liquid Reynolds number. The gas holdup is a strong function of the Froude number. The experimental values have been found to agree well the correlations.

Key words: Gas-liquid-solid fluidization; Pressure drop; Minimum fluidization velocity; Bed voidage; Gas holdup; Hollow cylindrical particles

1. Introduction

Gas-liquid-solid fluidization also known as three-phase fluidization is a subject of fundamental research since the last three decades due to its industrial importance. Three-phase fluidized beds have been applied successfully to many industrial processes such as in the H-oil process for hydrogenation and hydro-desulfurization of residual oil, the H-coal process for coal liquefaction, Fischer-Tropsch process, and the bio-oxidation process for wastewater treatment. Three-phase fluidized beds are also often used in physical operations [1]. The cocurrent gas-liquid flow in the three-phase fluidized bed with liquid continuous and gas in dispersed state is quite significant compared to other types [1, 2]. The co-current gas-liquid-solid fluidization is defined as an operation in which a bed of solid particles is suspended in upward flowing gas and/or liquid media due to the net gravitational force (i.e. gravitational force – buoyancy force) on the particles. Such an operation generates considerable intimate contact among the gas, liquid and solid particles in the system and provides substantial advantages for applications in physical, chemical or biochemical processing involving gas, liquid and solid phases [3].

The successful design and operation of a gas-liquid-solid fluidized bed system depends on the ability to accurately predict the fundamental characteristics of the system, viz. the hydrodynamics, the mixing of individual phases, and the heat and mass transfer characteristics [4-5]. Knowledge of minimum liquid fluidization velocity is essential for the successful operation of gas-liquid-solid fluidized beds. For such systems the minimum liquid fluidization velocity is the superficial liquid velocity at which the bed becomes fluidized for a given gas superficial velocity [6]. The minimum liquid flow rate required to achieve fluidization is determined by a plot of the bed pressure drop against the superficial liquid velocity at a constant gas flow rate and the corresponding liquid velocity is taken as the minimum liquid fluidization velocity [4]. Visual observation determines the minimum liquid fluidization velocity as either the velocity at which the bed first begins to expand or as the velocity at which any particle within the bed continuously shifts position with neighboring particles [7].

For chemical processes, where mass transfer is the rate-limiting step, it is important to be able to estimate the gas holdup since this relates directly to the rate of mass transfer [8-10]. The following equations have typically been used to determine the volume fraction (holdup) of each phase in a three phase fluidized bed:

$$\varepsilon_g + \varepsilon_l + \varepsilon_s = 1 \tag{1}$$

$$\frac{\Delta P}{\Delta H} = g(\rho_g \varepsilon_g + \rho_l \varepsilon_l + \rho_s \varepsilon_s) \tag{2}$$

$$\varepsilon_s = \frac{M_s}{\rho_s A_c H_e} \tag{3}$$

Where the bed height in Eq. (2) and (3) is obtained either visually or from the measured pressure drop gradient [1, 11]. A more direct method of measuring gas holdup is to simply isolate a representative portion of the test section by simultaneously shutting two quick closing valves and measuring the fraction of the isolated volume occupied by the

gas [2]. Other most promising methods of measuring the local gas holdup are electroresistivity and electro conductivity methods, γ - ray transmission measurements and radioactive tracer techniques [2-4, 12, 13].

In case of environmental applications of liquid-solid fluidized bed as anaerobic bioreactor and gas-liquid-solid fluidized bed as aerobic bioreactor for waste water treatment, a higher bed inventory is preferred as it increases the global depollution efficiency of the operation. Biological treatment is a slow process and needs long residence time for the waste water in the bed. Thus in this particular application, the design and operation of the fluidized bed should ensure a good quality of fluidization as well as sufficiently long residence time for the liquid (i.e. low liquid velocity). Sufficient contact time between micro-organisms and the pollutants is achieved in the system and maximum solid surface is available to the liquid. This emphasizes the study of the effect of bed mass on liquid-solid and gas-liquid-solid fluidization characteristics [14].

In the above cited literature the solid phase used is spherical particles: like glass beads, steel balls, plastic beads and other spherical catalyst particles, cylindrical particles: like aluminum cylinders and pvc cylinders other cylindrical catalyst particles and irregular particles like: sand, irregular gravel, quartz particles etc. having sphericity ranging from 0.7 – 1.0 approximately. Three-phase fluidized beds have been applied successfully in the bio-oxidation process for wastewater treatment in which various low-to-moderate density solid particles of different shape and size are used as cell support. In such reactors high surface area of the particle is desirable, which can be used as solid support for microorganisms, thus resulting in higher mass transfer rate. This can be achieved by the use of hollow cylindrical particles as, these possess very high surface to volume ratio i.e. of low sphericity.

In the present study have been conducted to examine the hydrodynamic behavior viz. the pressure drop, minimum liquid fluidization velocity, bed expansion and phase hold up of a co-current gas-liquid-solid three-phase fluidized bed with a modified air sparger using liquid as the continuous phase and gas as the discontinuous phase. Ceramic raschig rings having sphericity of 0.58 have been used as the solid phase as it is of moderate density and high surface to volume ratio due to its hollow cylindrical structure. These have been done in order to develop a good understanding of the gas holdup in low-moderate Reynolds number range. Correlation for minimum fluidization velocity, bed voidage and gas holdup have been developed from experimental data by dimensional analysis approach and compared with the correlation of Song et al. [15] and Safoniuk et al. [8] as they have used cylindrical particle as the solid phase.

2. Experimental Set-up and Techniques

A schematic representation of the experimental setup is shown in Fig. 1. The experimental fluidized bed consists of three sections, v.i.z., the test section, the gas-liquid distributor section, and the gas-liquid disengagement section. The test section is the main component of the fluidizer where fluidization takes place. It is a vertical cylindrical Plexiglas column of 0.1 m internal diameter and 1.88 m long. Any entrained particles are retained on the 16-mesh screen attached to the top of the column. The gas-liquid distributor is located at the bottom of the test section and is designed in such a manner that uniformly distributed liquid and gas mixture enters the test section. The distributor section made of Perspex is fructo-conical of 0.31 m in height, and has a divergence angle of 4.5^0 with one end of 0.0508 m in internal diameter and the other of 0.1 m in internal diameter. The liquid inlet of 0.0254 m in internal diameter is located centrally at the lower cross-sectional end. The higher cross-section end is fitted to the test section, with a perforated

plate made of G.I. sheet of 0.001 m thick, 0.12 m diameter having open area equal to 20 % of the column area with a 16 mesh (BSS) stainless steel screen in between. This has been done with a view to have less pressure drop at the distributor plate and a uniform flow of the fluids into the test section. There is an antenna-type air sparger of 0.09 m diameter just below the distributor plate containing 50 number of 0.001 m holes, for generating uniform bubbles to flow throughout the cross-section of the column. In this section the gas and liquid streams are merged and passed through the perforated grid. The mixing section and the grid ensured that the gas and liquid are well mixed and evenly distributed into the bed. The gas-liquid disengagement section at the top of the column is a cylindrical section of 0.026 m internal diameter and 0.034 m height, assembled to the test section with 0.08 m of the test section inside it, which allows gas to escape and liquid to be circulated through the outlet of 0.0254 m internal diameter at the bottom of this section.

For pressure drop measurement in the bed, the pressure ports have been fitted to the manometers filled with carbon tetrachloride. Pressure ports are available at seven different levels of equal spacing including one at bottom and one at the top of the test section. This has been done to measure the pressure drops at a particular section at three different radial positions viz. at the wall, at the center of the column and at one fourth of the diameter of the column from the wall. With this arrangement, the wall effect, distribution of particle concentration and the gas holdup can be studied clearly.

The three-phase solid, liquid and gas are ceramic raschig rings, tap water and the oil free compressed air respectively. The scope of the experiment is presented in Table 1. The air-water flow was co-current and upwards. Accurately weighed amount of material was fed into the column and adjusted for a specified initial static bed height. Water was pumped to the fluidizer at a desired flow rate using water flow meter. Then air was injected into the column through the air sparger at a desired flow rate using air flow meter.

Three calibrated flow meters with different ranges each for water as well as air have been used to accurately record the flow rates. Approximately five minutes was allowed to make sure that the steady state was reached. Then the readings of the manometers and the expanded heights of the bed was noted. For gas holdup measurement, the quick closing valves (9, Fig. 1) in the water and air line were closed simultaneously. At first free board experiment with wide variation of gas and liquid flow were conducted to calculate the two phase fractional gas hold up using Eq. (4).

$$\varepsilon_g = \left(\frac{H - H_l}{H} \right) \tag{4}$$

Similarly the gas holdup was calculated for the fluidization experiment with particles. The gas holdup in the three-phase region is calculated by subtracting the gas holdup in the two-phase region above the three-phase zone. The region above the expanded bed was the two-phase region. The values of minimum fluidization velocity for every run were obtained by plotting pressure drop across the bed against liquid flow rates at constant air flow rate. The procedure was repeated for different gas and liquid velocities at varying static bed heights.

3. Results and discussion

Experiments were conducted with the gas and liquid flow rates which varied from 0 - 0.127389 m/s and from 0 – 0.14862 m/s respectively. To ensure steady state in operation at least five minutes were allowed after which the readings for minimum fluidization, bed expansion, and gas holdup were noted down.

3.1. Pressure drop and minimum fluidization velocity

Fig. 2 shows the variation of pressure drop with superficial liquid velocity in gas-liquid-solid system for different initial static bed heights. The experimental pressure drops found are very close to that can be obtained from basic force balance in two phase fluidization, which indicates no wall effect to fluidization in this case. As the ratio of column diameter to the equivalent diameter of the pipe is 14.5 wall effects is not expected, wall effect is prominent when the ratio is less than 8. The pressure drop obtained from manometer reading for a three phase system does not represent the true frictional drag on the solid particles which holds the particles in suspended conditions as the hydrostatic pressure in the column changes due to gas holdup. On the other hand the pressure drop measurement is used to calculate the phase holdup in the bed.

The minimum fluidization velocity in this study was obtained from the plot of pressure drop and superficial liquid velocity. Some researchers have shown the variation of minimum fluidization velocity with the bed mass (or initial static bed height) which is an uncommon phenomenon [14]. In the present case the effect of bed mass on minimum liquid fluidization velocity has been studied as represented in Fig. 2. It is observed that bed mass (or initial static bed height) has no effect on minimum fluidization velocity. At all the bed heights the minimum liquid fluidization velocity has been found to be 0.02654 m/s. which agrees well with the detailed study on the effect of column diameter and initial static bed height on the minimum fluidization velocity in a three-phase fluidized bed by Begovich and Watson [4]. Since fluidization of a bed is achieved when the upward inertial and drag forces exerted on the particles by the fluids equal the buoyant weight of the bed, an effect of static bed height on the minimum fluidization velocities would only be expected if end effects were present in the bed.

The pressure drop profile with variation of superficial liquid velocity for gas-liquid-solid system at different constant superficial gas velocities shown in Fig. 3. From

this pressure drop profile the minimum liquid fluidization velocity has been determined. It can be seen from this figure that the minimum liquid fluidization velocity decreases with the gas velocity. The decrease in minimum liquid fluidization velocity may be due the contribution of the gas to the total drag on the particles by the gas-liquid up ward flow. The relative velocity may promote fluidization at a lower liquid fluidization velocity. Fig. 4 shows the variation of minimum liquid fluidization velocity ($V_{lmf)}$ with superficial gas velocity. It can be seen from the figure that the rate of decrease in minimum liquid fluidization velocity is large at lower gas velocity but the rate decreases as gas velocity increases. The sharp decrease in minimum liquid fluidization velocity with introduction of the gas indicates the bubble supported fluidization in presence of gas, but with increase in the gas velocity the contribution of the gas to fluidization decreases. In the present study continuous decrease in V_{lmf} is observed whatever small the change may be. Briens et al [6] have reported a little different trend. According to them the decrease in V_{lmf} is large at lower gas velocity but the rate decreases as gas velocity increases, however at higher gas velocity; the minimum liquid fluidization velocity becomes almost constant

The minimum liquid fluidization velocity for liquid-solid fluidization is within 5% that predicted from the correlation of Wen and Yu [16] marked as short horizontal line in Fig. 4. Song et al. [15] have experimentally predicted the minimum liquid fluidization velocity by pressure gradient method for cylindrical hydrotreating catalysts in a three-phase fluidized bed. They have proposed a correlation given by Eq. (5) for the prediction of V_{lmf} in a three-phase fluidized bed with cylindrical particles.

$$\frac{V_{lmf}}{V_{lmf}^{ls}} = 1 - 376 V_g^{0.327} \mu_l^{0.227} d_e^{0.213} (\rho_s - \rho_l)^{-0.423} \tag{5}$$

In the present work as hollow cylindrical particles have been used as the solid phase, the same correlation given by Eq. (5) has been used to calculate the V_{lmf}. The

calculated values of V_{lmf} from Eq. (5) using the equivalent diameter have been compared in Fig. 4. Very close agreement is seen between the calculated and the experimental values. In some cases both the values are found to be almost same. Here a correlation for minimum liquid fluidization velocity has been developed in dimensional form. The parameters of importance are gas velocity, particle size, column diameter, static bed height, and density of solid, liquid and gas. In this experiment except in the variation of gas velocity and static bed height, other parameters have been kept constant. As from the above results it is observed that bed mass (initial static bed height) has no effect on minimum liquid fluidization velocity, only the relation between V_{lmf} and superficial gas velocity V_g will therefore be in the form

$$V_{lmf} = 0.0049(V_g)^{-0.5182} \quad (6)$$

(with a correlation factor of 0.9564 and standard deviation of 0.0698).

By using this correlation given by Eq. (6) the V_{lmf} have been calculated for different gas velocities and have been compared with their respective experimental values. The values calculated from correlation have been found to agree well with the experimental values with standard and mean deviation of 0.06975 and 0.06014 respectively. Thus, the correlation given by Eq. (6) can be used for such system to predict the V_{lmf} at all gas velocities except the zero gas velocity.

3.2. Bed voidage

The expanded bed height was measured by visual observation and the data were compared with the pressure drop profile along the length of the column measured by a number of manometers. Fairly good agreement was observed between two measurements. The bed expansion study carried out by varying liquid velocity (at a constant gas velocity)

has been presented in terms of bed expansion ratio in Fig. 5. It is seen from the figure that the bed expansion ratio increases with increase of both the liquid and the gas velocities.

The bed voidage or bed porosity is defined as the fraction of the bed volume occupied by both liquid and gas phases and as such directly proportional to the expanded bed height. As in the present study hollow cylindrical particles have been used as the solid phase, the bed expansion simply does not relate to the bed voidage unless the hollow volume is taken into account. The bed voidage has been calculated by considering the hollow volume and has been represented graphically in Fig. 6 for the conditions above the minimum fluidization. Song et al. [15] have rewritten the original Begovich and Watson [4] correlation by introducing shape factor term for calculation of bed voidage of cylindrical particles in three-phase fluidized bed with air and water as the gas and the liquid phases respectively. The correlation of song et al. [15] is given as under:

$$\varepsilon = 3.93\phi_s^{-0.424} V_l^{0.271} V_g^{0.0410} \mu_l^{0.0550} d_e^{-0.268} D_c^{-0.0330} (\rho_s - \rho_l)^{-0.316} \quad (7)$$

The bed voidage for the three-phase fluidized bed calculated from the above equation has been presented graphically in Fig. 6. Bed voidage both experimental and calculated from Eq. (7) have been plotted against superficial liquid velocity at different constant gas velocities. It is clear from this that the bed voidage increases with increase of both the liquid velocity and the gas velocity. The bed voidage is a strong function of liquid velocity, but is a weak function of gas velocity. For almost all cases the experimental bed voidage is found to be less than that is predicted from Eq. (7). There is higher deviation between the values at lower liquid velocities but close agreement is seen for higher liquid velocities. This may be due to the fact that the correlation developed by song et al. [15] is from their experimental bed voidage obtained at higher gas and liquid velocities than the present study. This indicates the correctness of Eq. (7) for predicting bed voidage at higher gas and liquid velocities where the bed expansion ratio is nearly greater than 2.5. In Fig. 7

the plot of bed voidage (experimental and calculated from Eq. (7)) vs. bed expansion ratio shows the same trend. A singe line for experimental bed voidage is seen in the figure for all gas velocities as the former has been calculated from the experimental bed expansion ratio. Fig. 8 shows the variation of bed voidage with the ratio of superficial liquid to gas velocity. It is clear from the plot that for higher gas velocities (liquid to gas velocity ratio <1.5), there exists very close agreement between the experimental bed voidage and that calculated from Eq. (7).

A simple correlation has been developed from the experimental data of bed voidage above the minimum fluidization condition upto the expanded bed height of about 3.5 times that of the initial static bed height. In this experiment the particle size, sphericity and density of the solid, viscosity and density of liquid, and column diameter are constant. Thus the bed expansion or bed voidage determined here is a simple function of gas and liquid velocities and initial static bed height. Fig. 9 is the plot of the variation of bed expansion ratio with superficial liquid velocity at a constant gas velocity for different initial static bed heights. It is clear from the plot that the bed voidage is not a function of the initial static bed height as the bed expansion ratio is more or less same for all the cases. Thus the bed voidage for this case is a function of gas and liquid velocities only and can be written as in the range of 0.0425 m/s $\leq V_l \leq$ 0.1380 m/s and 0.0212 m/s $\leq V_g \leq$ 0.1062 m/s, this leads to:

$$\varepsilon = 3.29 V_l^{0.4220} V_g^{0.1469} \tag{8}$$

(with a standard deviation of 0.02483, mean deviation of 0.01910 and a correlation coefficient of 0.9701)

The bed voidage values calculated from Eqs. (7) and (8) are compared with the experimental ones in Fig. 10. Fairly good agreement is seen between the experimental values and with those calculated by both the equations for air-water system. More than

65% of the data of Song et al. [15] and all values from present correlation are within 10%. Where as all the values from Eq. (7) is within 20% but with almost positive deviation from experimental ones.

Fig. 11 shows the variation of bed voidage with superficial gas velocity at minimum fluidization. The minimum fluidization condition has been determined from pressure drop profile and the bed height by visual observation. Then the bed voidage has been calculated from bed height at minimum fluidization. It is clear from the plot that bed voidage of three-phase bed is less than that of the liquid-solid bed for all gas velocities. At the introduction of the gas the bed voidage is first reduced and then with increase of the gas velocity it increases. Kim et al [11] have shown a continuous increase in bed voidage for 6 mm glass beads and 2.6 mm irregular gravels, but decrease in bed voidage for 1mm glass beads for air-water system. It is indicated from the figure that in the presence of gas phase a more compact bed is possible than in two-phase liquid solid system. The injection of small amount of gas causes the bed to collapse, but with increase in gas velocity the bed voidage again increased. The increasing trend is same as of Kim et al. [11] for large particles as with increase of gas velocity the bubble size increases.

3.3 Gas holdup

Fig. 12 shows the variation of fractional gas holdup with superficial liquid velocity at different values of fixed superficial gas velocity. It is seen from the figure that with increasing liquid velocity, the gas holdup decreases. However the variation of fractional gas holdup with liquid velocity is very small. Several workers have reported that the fractional gas holdup is practically unaffected by liquid velocity except at very high liquid superficial velocities [8]. According to Dhanuka and Stepanek [3] and Song et al. [15]

there is a slight decrease in gas holdup with liquid velocity [3, 15]. This may possibly be due to the lower residence time of the gas bubbles in the bed at higher liquid velocities.

Fig. 13 represents the variation of fractional gas holdup with superficial gas velocity, at constant liquid velocities. As seen from the figure, the fractional gas holdup increases monotonically with the gas velocity with relatively higher values of the slope at low gas velocities. This corroborates the findings of Dhanuka and Stepanek [3] and Safoniuk et al. [8]. In lower range of gas velocity, an increase in gas velocity results in the formation of a larger number of gas bubbles without appreciable increase in the bubble diameter. Therefore an increasing fractional gas holdup is observed. As gas velocity increases the bubble size grows due to bubble coalescence, and relatively the gas holdup decreases. As the experiment has been conducted for the gas velocity range pertaining to the distributed bubble regime, the decrease in slope is not significant which is observed for the transformation to the slug flow regime.

In air-water systems, both coalesced bubbling and dispersed bubbling regime are observed and the gas holdup behaviour strongly depends upon the flow regime. In the present experimental range of gas liquid velocities mainly dispersed bubbling regime is observed. For dispersed bubbling regime, the gas holdup in three-phase fluidized beds containing cylindrical catalysts, correlation in terms of gas particle Froude number (Fr_g) and the liquid particle Reynolds number (Re_l) has been proposed by Song et al. [15], which is given by the following correlation (Eq. (9)).

$$\varepsilon_g = 0.280 Fr_g^{0.126}\, \mathrm{Re}_l^{-0.0873} \tag{9}$$

This correlation predicts much lower value of gas holdup than the experimental ones as shown in Figs. 14 and 15. At low gas velocity the gas holdup calculated from Eq. (9) is close to experimental value, but as the gas velocity increases the deviation becomes more and more. The latest correlation for predicting gas holdup available in literature for

cylindrical solid particles is by Safoniuk et al. [8]. They have proposed the correlation for gas holdup in terms of modified gas Reynolds number (Re_g), which is given by Eq. (10).

$$\varepsilon_g = 0.014 * \mathrm{Re}_g^{\,0.426} \tag{10}$$

Gas holdup predicted from Eq. (10) has been compared with that obtained from the present experiment in Figs. 14 and 15. It is seen from Fig. 14 that Eq. (10) predicts the gas holdup higher than the experimental ones at lower gas velocities, but close agreement is there at higher gas velocities. As both the correlations are not accurately predicting the gas holdup for hollow cylindrical particles for the present range of experiments, a correlation in the form of Eq. (9) has been proposed here from the experimental data to predict the gas holdup. For this the results have been fitted to a power-law equation passing through origin (zero gas holdup at zero gas flow). For the range of $362.275 \leq \mathrm{Re_l} \leq 905.772$ and $0.0067 \leq \mathrm{Fr_g} \leq 0.1674$, this leads to:

$$\varepsilon_g = 1.3567 Fr_g^{0.3835}\, \mathrm{Re}_l^{-0.1466} \tag{11}$$

(with a standard deviation of 0.039 and a correlation coefficient of 0.994).

Close agreement between the gas holdup predicted from Eq. (11) and experimental ones is seen from Figs. 14 and 15. From the experimental data some are taken for the development of correlation as Eq. (11). Rest of the experimental data along with those used for developing the correlation has been compared with those of the calculated values of gas holdup from Eq. (11). More than 95% are within 10%, where as all are within 20%. This shows a very good agreement and the significance of the developed correlation. Except at lower gas velocities i.e. at lower gas hold up range for all other cases the predicted gas holdup from Eq. (10) of Safoniuk et al. [8] is within 20% deviation from the developed correlation. The reverse trend is shown by Eq. (9) of Song et al. [15] i.e. the predicted gas holdup except for the lower range have a negative deviation of more than 20% and the deviation increases at higher values of gas holdup.

4. Conclusions

Bed pressure measurement, a standard technique gives the minimum liquid fluidization velocity in the range of 0.06344 to 0.01485 m/s**,** which continuously decreases with superficial gas velocity over range of experimental conditions. The bed voidage has been found to increase with both gas and liquid velocities in the fluidization regime. The bed voidage at minimum fluidization is found to be 0.54586 for liquid-solid fluidization, which suddenly decreases with the introduction of the gas. Later with increase in gas velocity the bed voidage increases, but for all cases the bed voidage at minimum fluidization in three-phase has been found to less than the liquid-solid bed. The gas holdup increases with gas velocity and decreases with liquid velocity but is a weak function of the latter. The experimental data and the developed correlations may be useful for better understanding of the behaviour of a gas-liquid-solid fluidized bed system using hollow cylindrical particles as the solid phase.

Appendix A. Nomenclature

A_c cross-sectional area of the column (m^2)

d_e equivalent diameter of particle (m)

D_c column diameter (m)

Fr_g gas particle Froude number (U_g^2/d_eg)

g acceleration due to gravity (m/s^2)

H total height of test section (m)

H_l height of the liquid in the column after the escape of gas (m)

H_e height of expanded bed (m)

H_s initial static bed height (m)

M_s mass of the solid in the bed (kg)

$\frac{\Delta P}{\Delta H}$ pressure gradient in the bed (Pa/m)

R bed expansion ratio (H_e/H_s)

Re_l particle liquid Reynolds number ($\rho_l V_l d_p/\mu_l$)

Re_g modified gas Reynolds number (β_u* Re_l)

V_l liquid velocity (m/s)

V_g gas velocity (m/s)

V_{lmf} minimum liquid fluidization velocity for a three-phase system (m/s)

V^{ls}_{lmf} minimum liquid fluidization velocity for liquid-solid system (m/s)

Greek symbols

ε bed voidage

$\varepsilon_g, \varepsilon_l, \varepsilon_s$ fractional gas, liquid and solids holdup respectively

β_u ratio of superficial velocities (V_g/ V_l)

ρ_g, ρ_l, ρ_s gas, liquid and particle density (kg/m^3)

μ_l liquid viscosity (Pa.s)

Subscripts

l liquid phase

g gas phase

s solid phase

References

[1] K. Muroyama, L.S. Fan, Fundamentals of gas-liquid-solid fluidization, AIChE. J. 31 (1985) 1-34.

[2] N. Epstein, Three-phase fluidization: Some knowledge gaps, Can. J. Chem. Eng. 59 (1981) 649-757.

[3] V.R. Dhanuka, J.B. Stepanek, Gas and liquid hold-up and pressure drop measurements in a three-phase fluidized bed, in: Fluidization, J.F. Davison, D.L. Keairns (Eds.), Cambridge University Press, UK, 1978, pp. 179-183.

[4] J.M. Begovich, J.S. Watson, Hydrodynamic characteristics of three-phase fluidized beds, in: Fluidization, J.F. Davison, D.L. Keairns (Eds.), Cambridge University Press, Cambridge, 1978, pp.190-195.

[5] T.J. Lin, C.H. Tzu, Effects of macroscopic hydrodynamics on heat transfer in a three-phase fluidized bed, Catalysis Today 79–80 (2003) 159–167.

[6] L.A. Briens, C.L. Briens, A. Margaritis, J. Hay, Minimum liquid fluidization velocity in gas-liquid-solid fluidized beds, AIChE J. 43 (1997) 1180-1189.

[7] L.A. Briens, C.L. Briens, A. Margaritis, J. Hay, Minimum liquid fluidization velocity in gas-liquid-solid fluidized beds of low-density particles, Chem. Eng. Sci. 52 (1997) 4231-4238.

[8] M. Safoniuk, J.R. Grace, L. Hackman, C.A. Mcknight, Gas hold-up in a three-phase fluidized bed, AIChE J. 48 (2002) 1581-1587.

[9] J.M. Schweitzer, J. Bayle, T. Gauthier, Local gas hold-up measurements in fluidized bed and slurry bubble column, Chem. Eng. Sci. 56 (2001) 1103–1110.

[10] L.S. Fan, F. Bavarian, R.I. Gorowara, B.E. Kreischer, Hydrodynamics of gas-liquid-solid fluidization under high gas hold-up conditions, Powder Technol. 53 (1987) 285 -293.

[11] S.D. Kim, C.G.J. Baker, M.A. Bergougnou, Phase holdup characteristics of three-phase fluidized beds, Can. J. Chem. Eng. 53 (1975) 134-139.

[12] V.K. Bhatia, N. Epstein, Three phase fluidization: A generalized wake model, in: Fluidization and its applications, H. Angelino et al. **(**Eds.), Cepadues Editions, Toulouse, 1974, pp. 380-392.

[13] H. Yu, B.E. Rittman, Predicting bed expansion and phase hold-up for three-phase fluidized bed reactors with and without biofilm, Water Res. 31 (1997) 2604-2616.

[14] A. Delebarre, J. M. Morales, L. Ramos, Influence of bed mass on its fluidization characteristics, Chem. Eng. J. 98 (2004) 81-88.

[15] G. H. Song, F. Bavarian, L. S. Fan, Hydrodynamics of three-phase fluidized bed containing cylindrical hydrotreating catalysts, Can. J. Chem. Eng. 67 (1989) 265-275.

[16] C. Y. Wen and Y. H Yu, Mechanics of Fluidization, Chem. Eng. Symp. Ser., 62 (62) (1966), 100-111.

Figure captions.

Fig. 1. Schematic representation of the three-phase fluidized bed.

Fig. 2. Variation of bed pressure drop with liquid velocity for different static bed heights at V_g = 0.06369 m/s.

Fig. 3. Variation of bed pressure drop with liquid velocity for different gas velocities at H_s = 0.214 m.

Fig. 4. Variation of minimum liquid fluidization velocity with gas velocity.

Fig. 5. Variation of bed expansion ratio with liquid velocity for different gas velocities at H_s = 0.214 m.

Fig. 6. Variation of bed voidage with liquid velocity for different gas velocities at H_s = 0.214 m.

Lists of Tables

Table 1

Scope of the experiment

A. Properties of bed materials				
Materials	**L = OD, m**	**ID, m**	**Spherical volume-equivalent diameter, m**	**ρ_p (kg/m^3)**
Ceramic raschig ring	0.0066	0.0033	0.006864	1670
Initial static bed height (m)	0.154	0.214	0.264	0.314
B. Properties of fluidizing medium			**ρ (kg/m^3)**	**μ (Pa.s)**
Air at 25^{0}C			1.187	0.0000181
Water at 25^{0}C			997.15	0.000891
C. Properties of manometric fluid			**ρ (kg/m^3)**	**μ (Pa.s)**
Mercury			13,574	0.001526
Carbon tetra-chloride (CCl_4)			1,600	0.000942

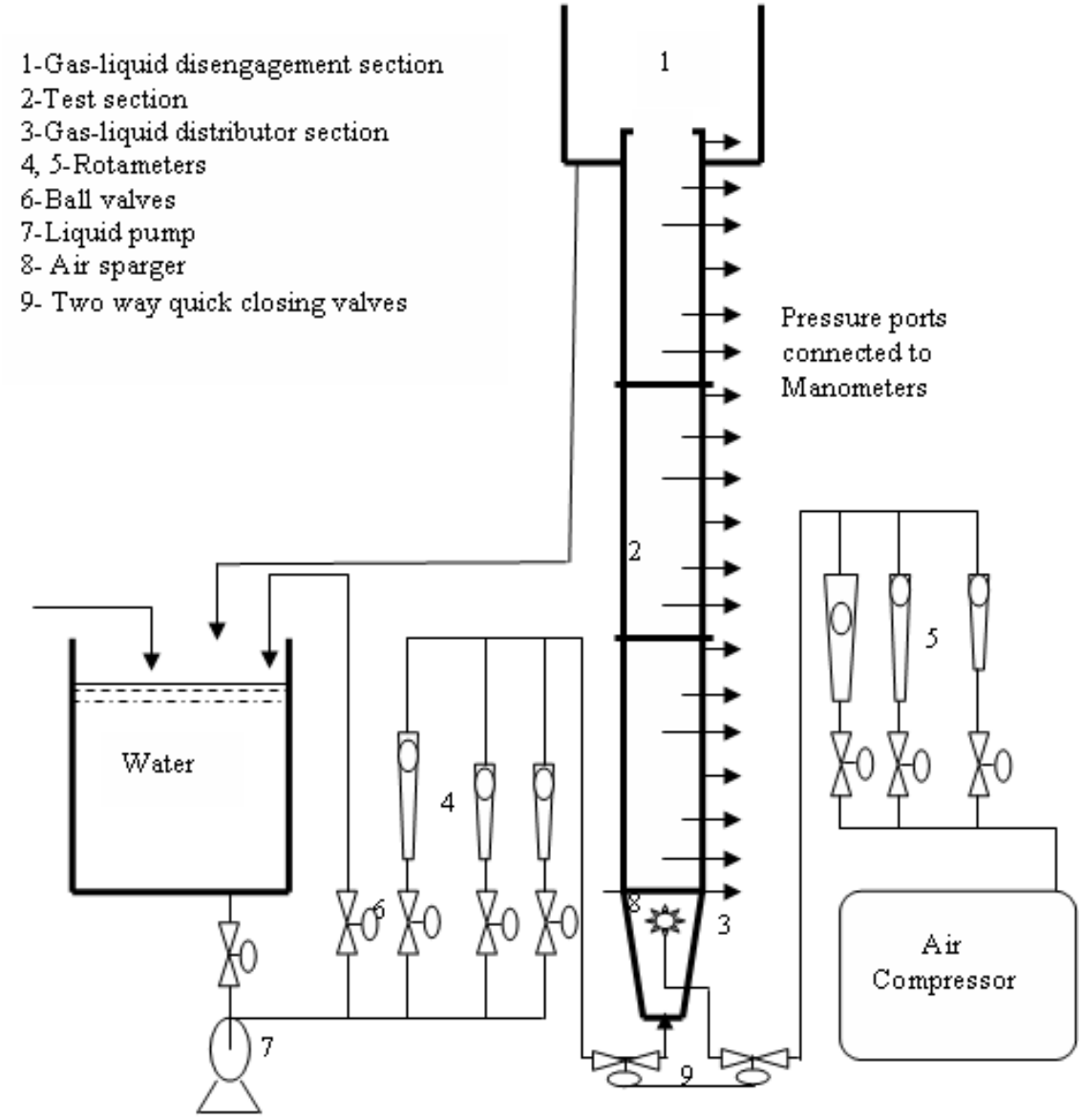

Fig. 1. Schematic representation of the three-phase fluidized bed.

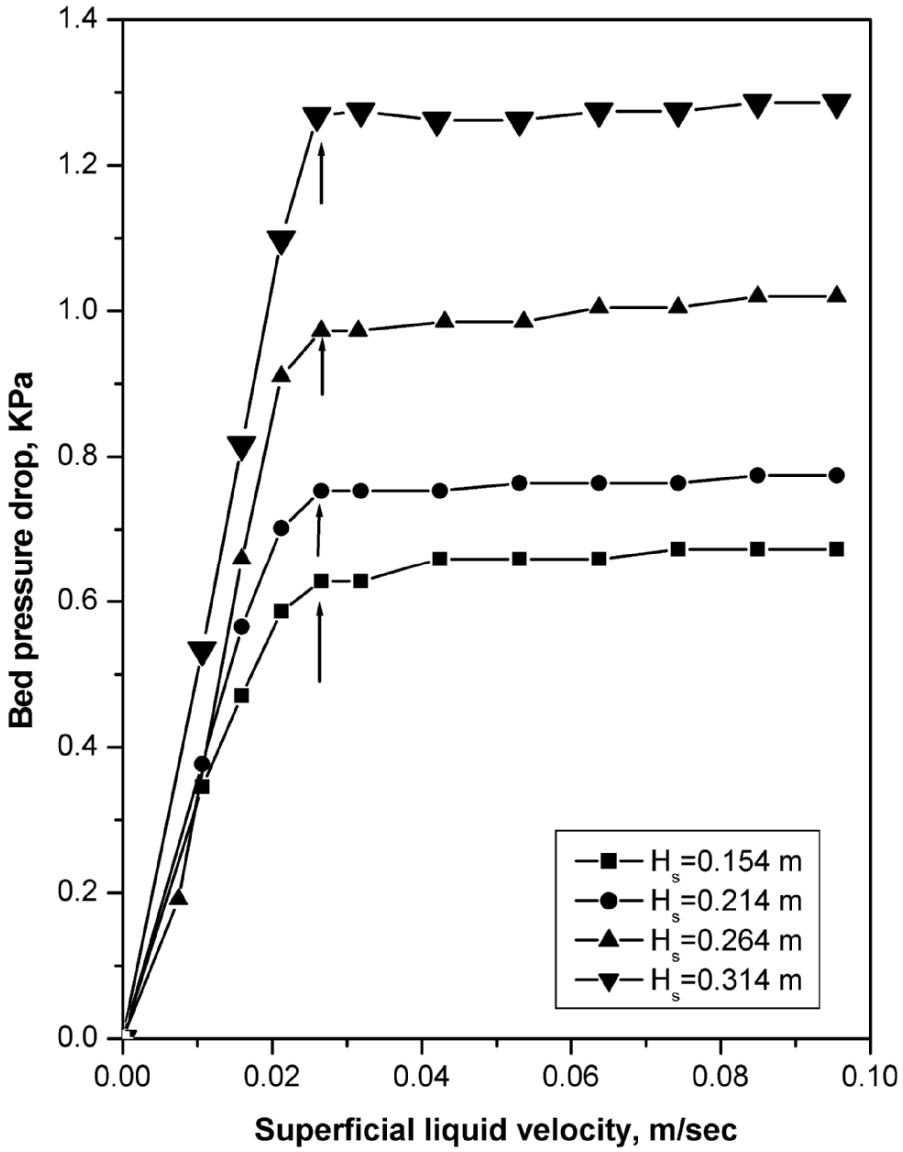

Fig. 2. Variation of bed pressure drop with liquid velocity for different static bed heights at V_g = 0.06369 m/s.

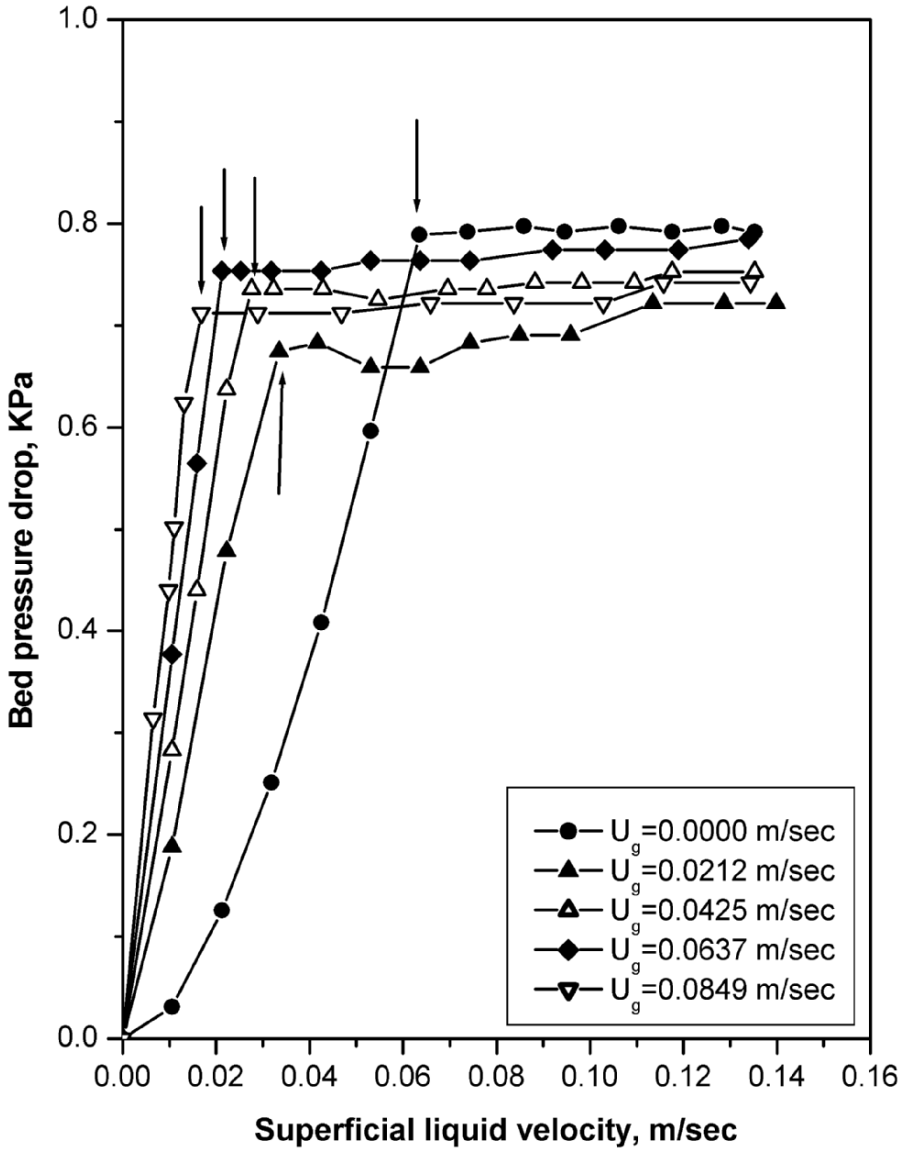

Fig. 3. Variation of bed pressure drop with liquid velocity for different gas velocities at H_s = 0.214 m.

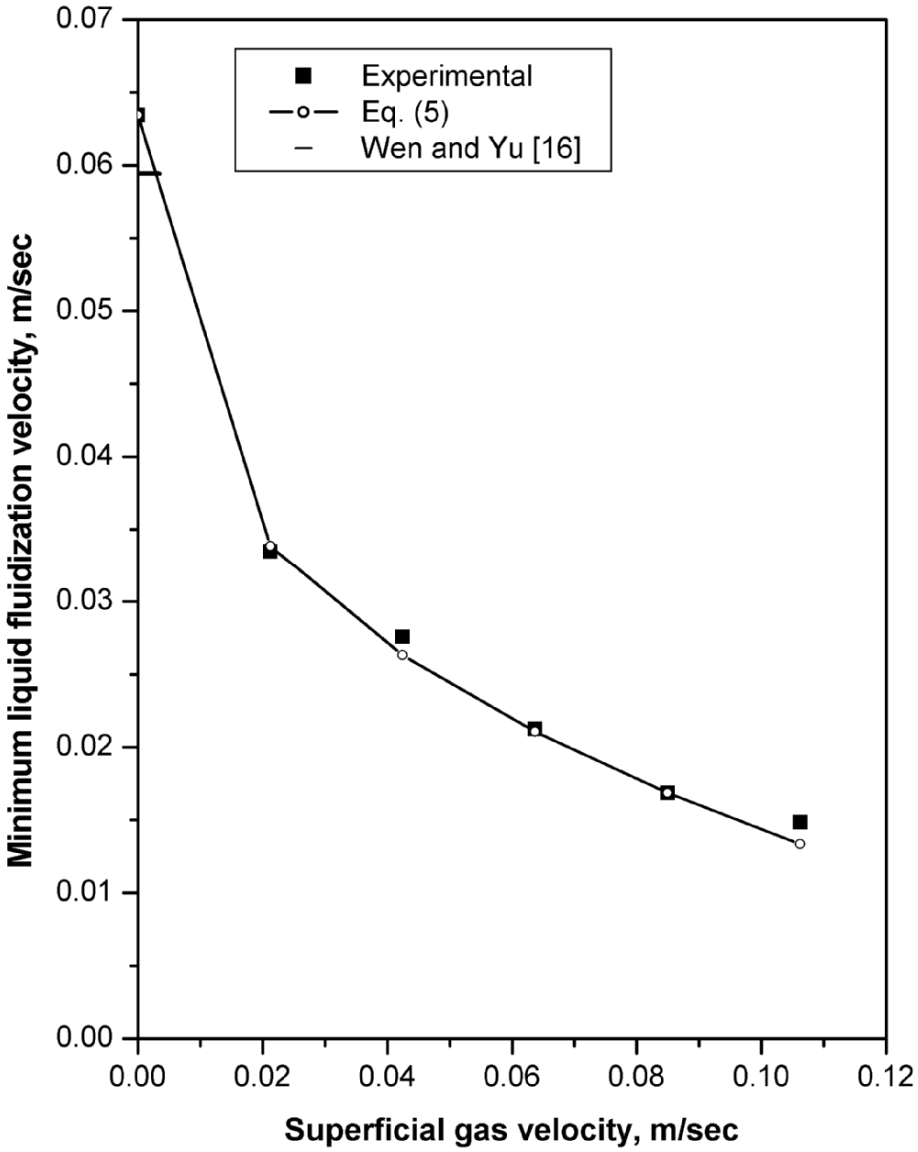

Fig. 4. Variation of minimum liquid fluidization velocity with gas velocity.

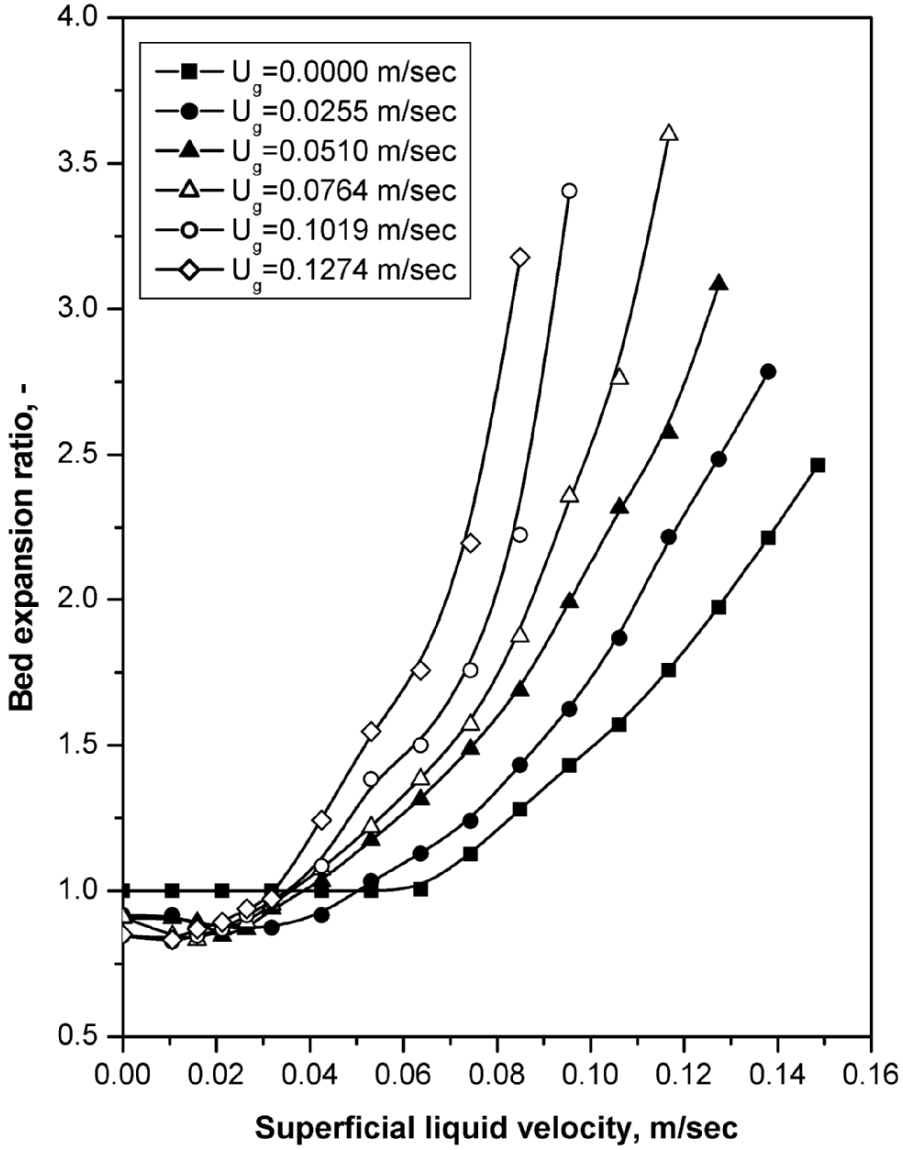

Fig. 5. Variation of bed expansion ratio with liquid velocity for different gas velocities at $H_s = 0.214$ m.

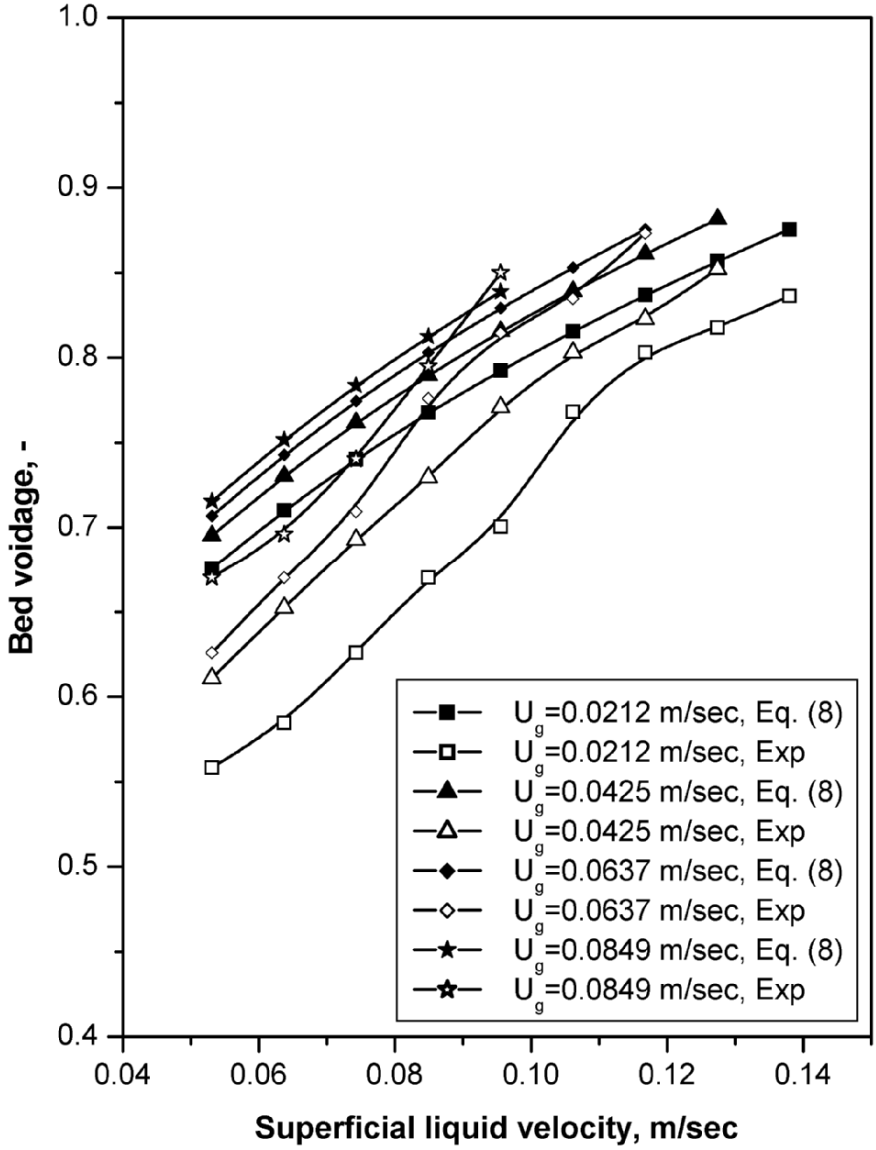

Fig. 6. Variation of bed voidage with liquid velocity for different gas velocities at H_s = 0.214 m.

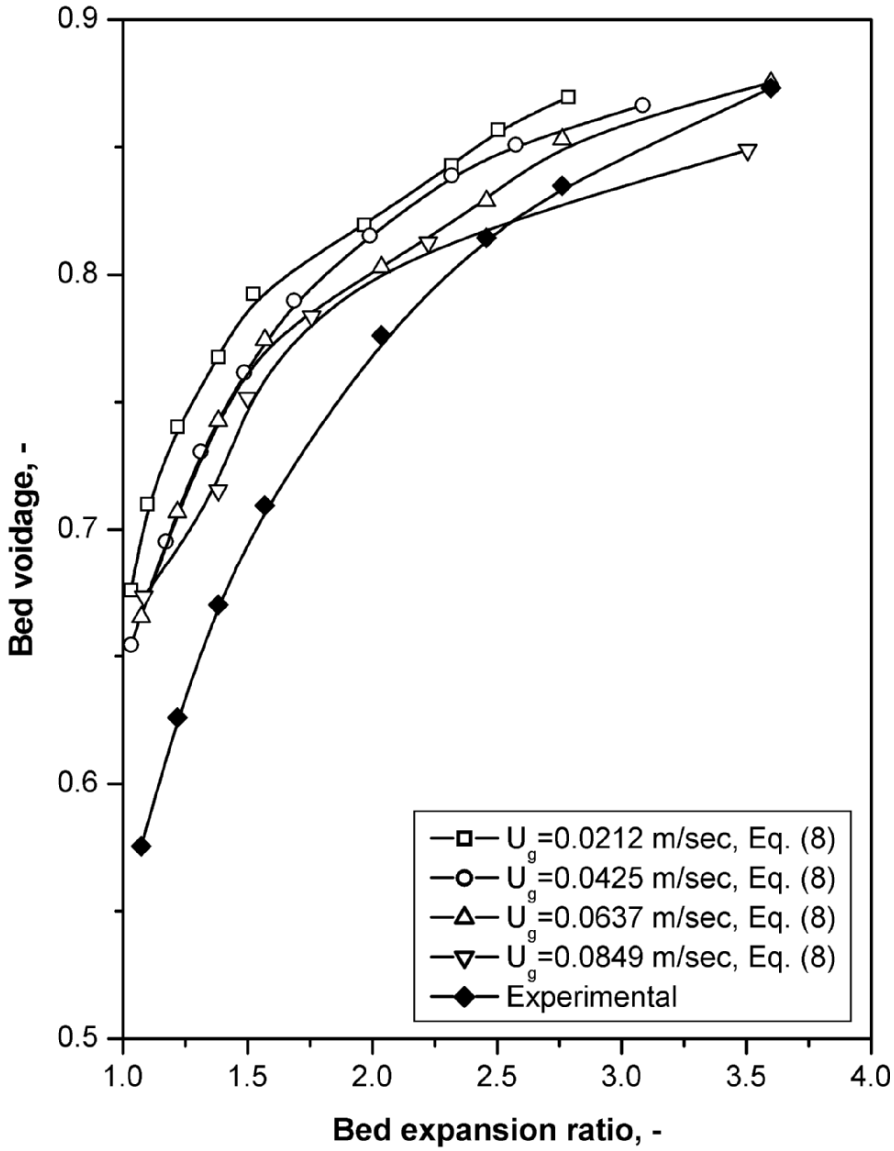

Fig. 7. Variation of bed voidage with bed expansion ratio for different gas velocities at H_s = 0.214 m.

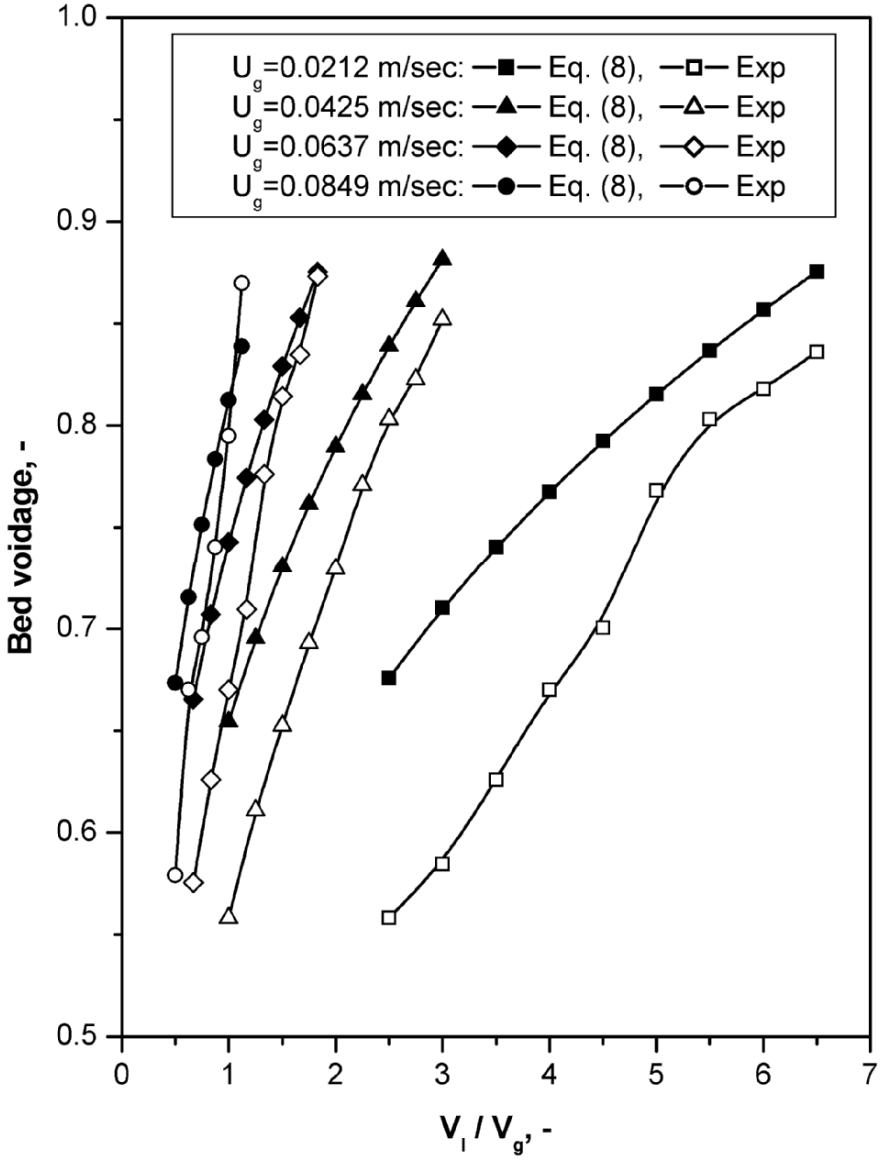

Fig. 8. Variation of bed voidage with ratio of liquid to gas velocity for different gas velocities at $H_s = 0.214$ m.

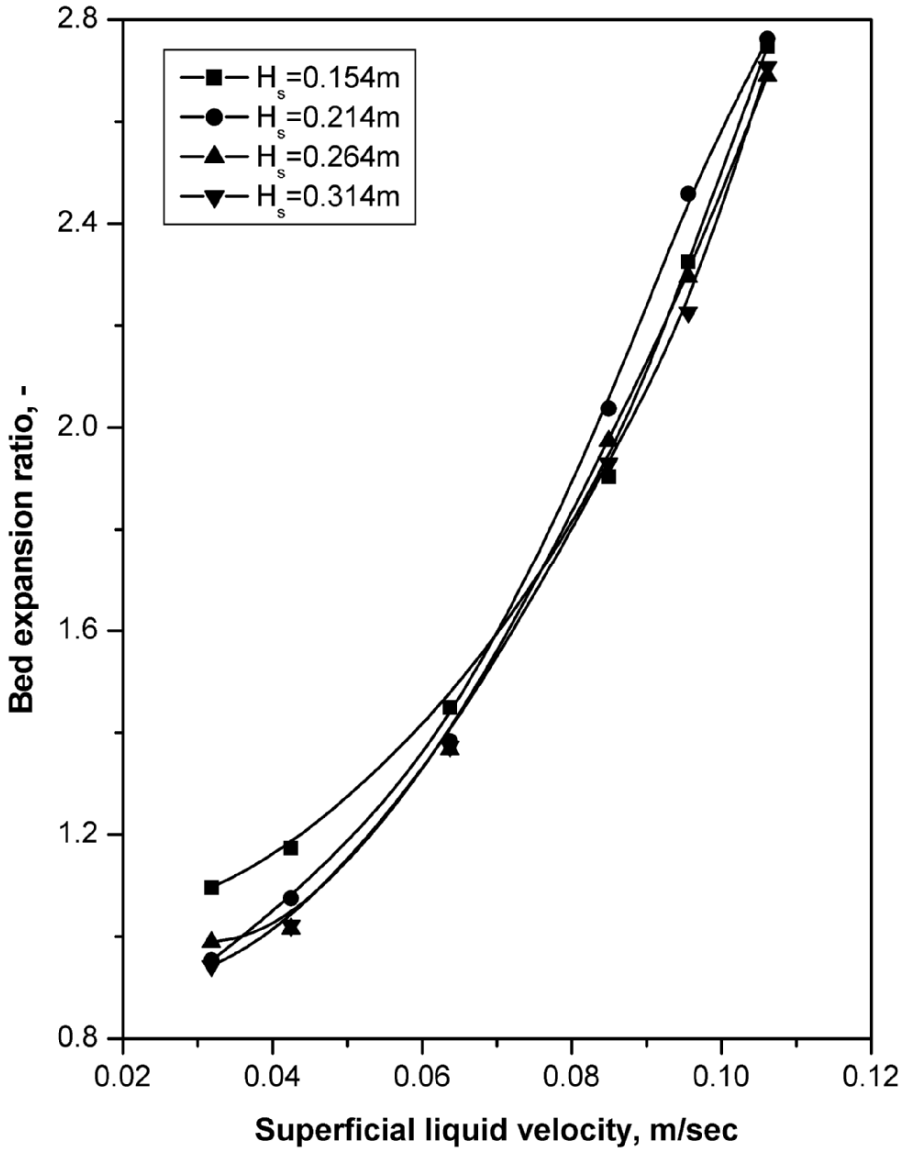

Fig. 9. Variation of bed expansion ratio with liquid velocity for different initial static bed heights at gas velocity of 0.0637 m/s.

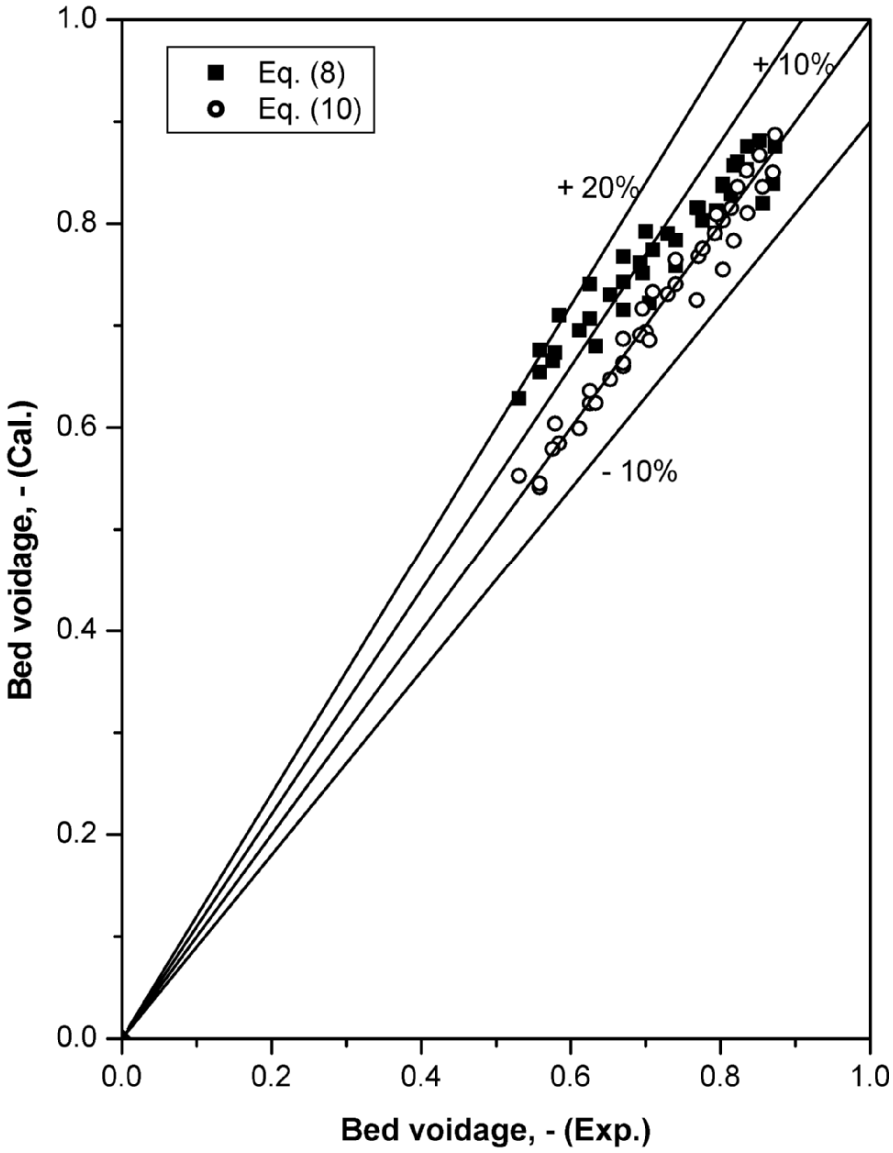

Fig. 10. Comparison of calculated values of bed expansion ratio from Eqs. (7) and (8) with the experimental values.

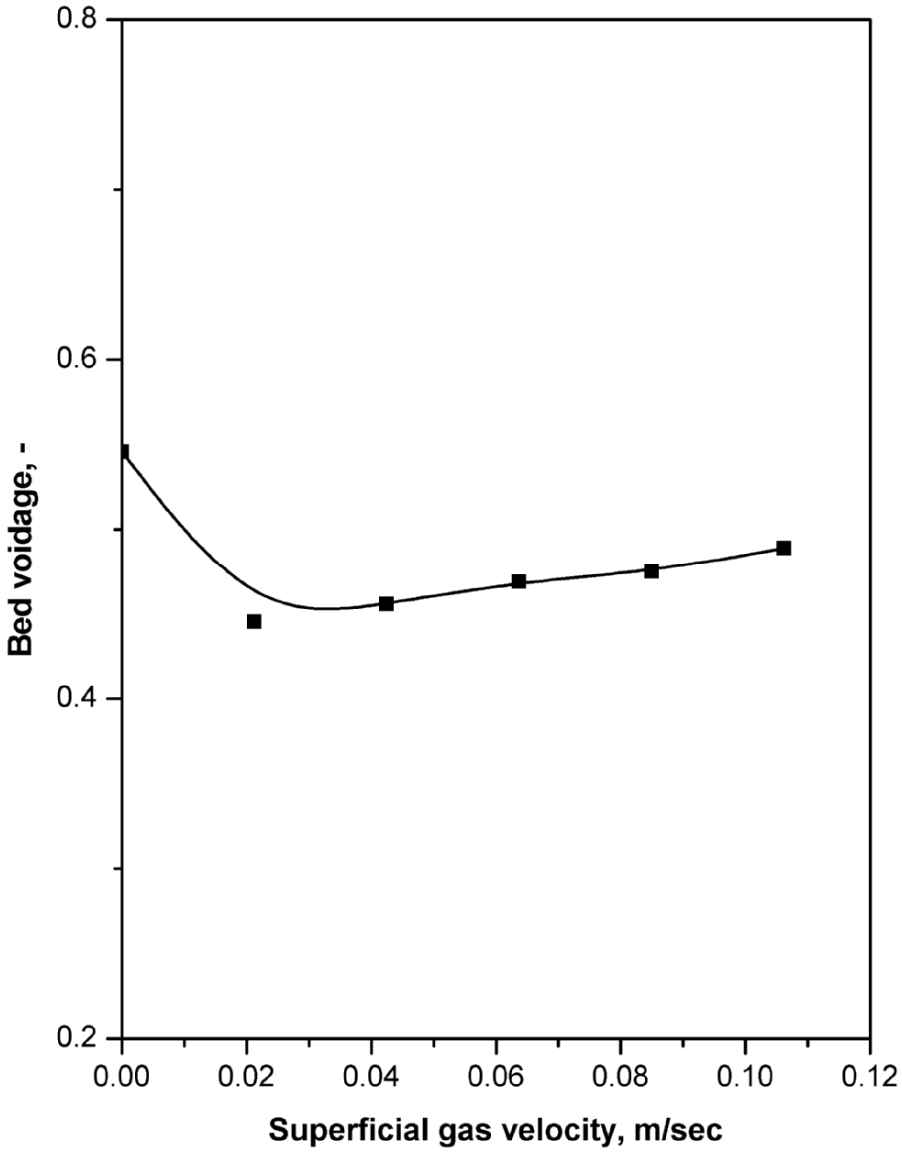

Fig. 11. Variation of bed voidage with gas velocity at minimum fluidization at $H_s = 0.214$ m.

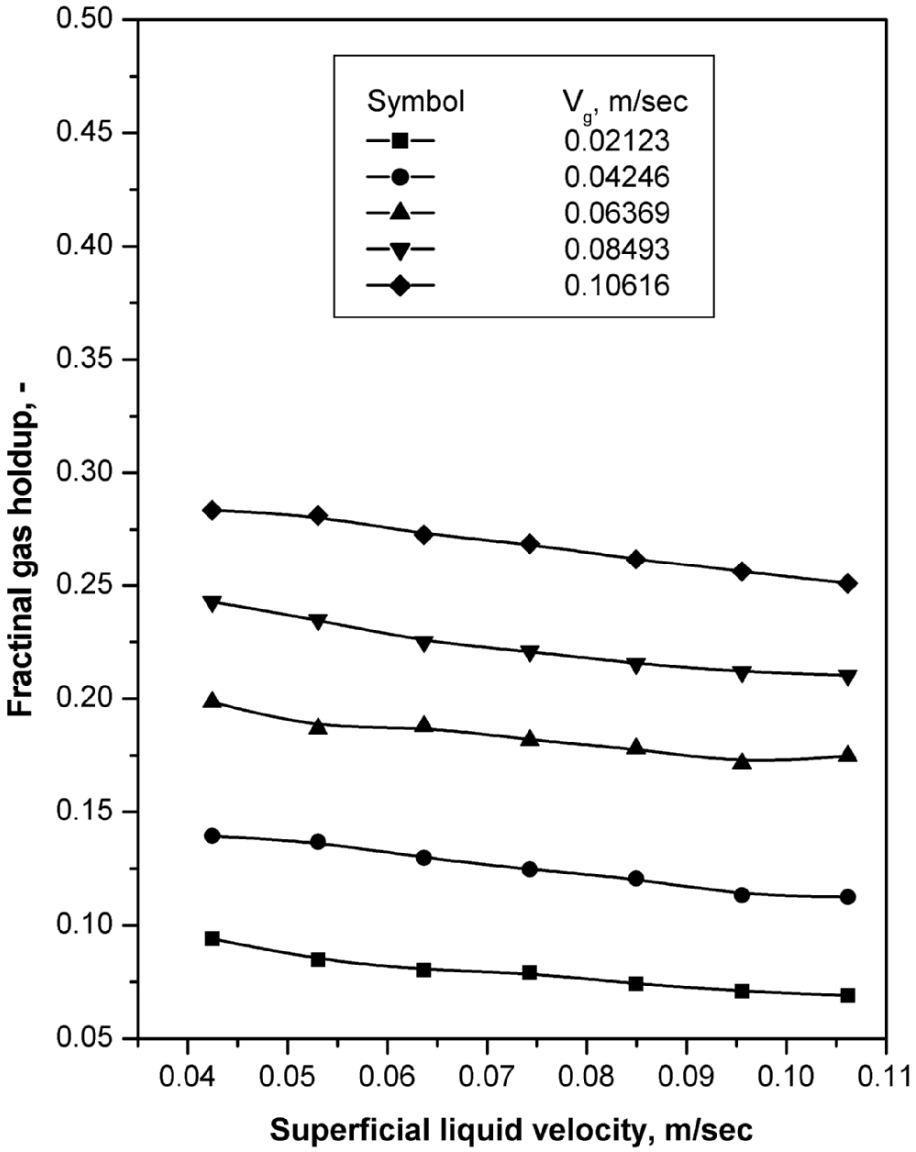

Fig. 12. Variation of gas holdup with liquid velocity for different gas velocities at H_s = 0.214 m.

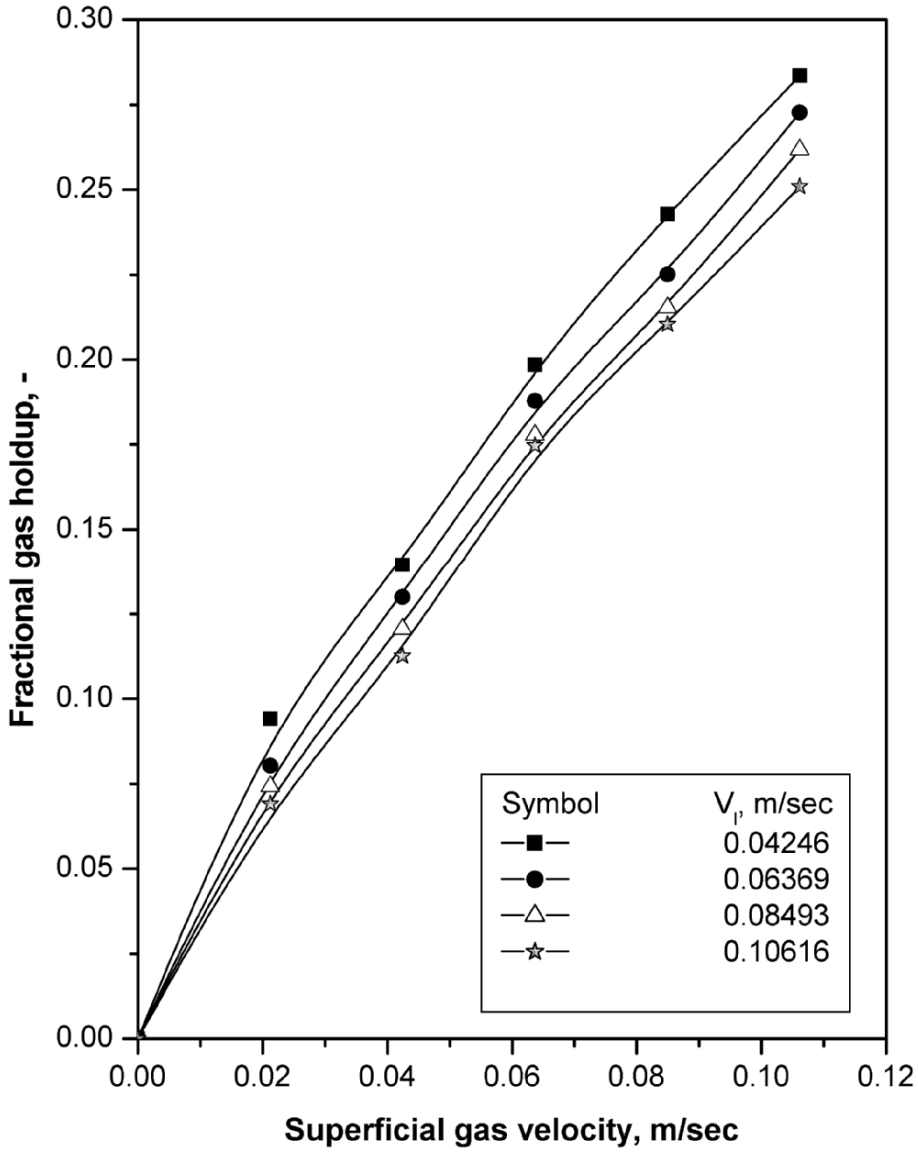

Fig. 13. Variation of gas holdup with gas velocity for different liquid velocities at H_s = 0.214 m.

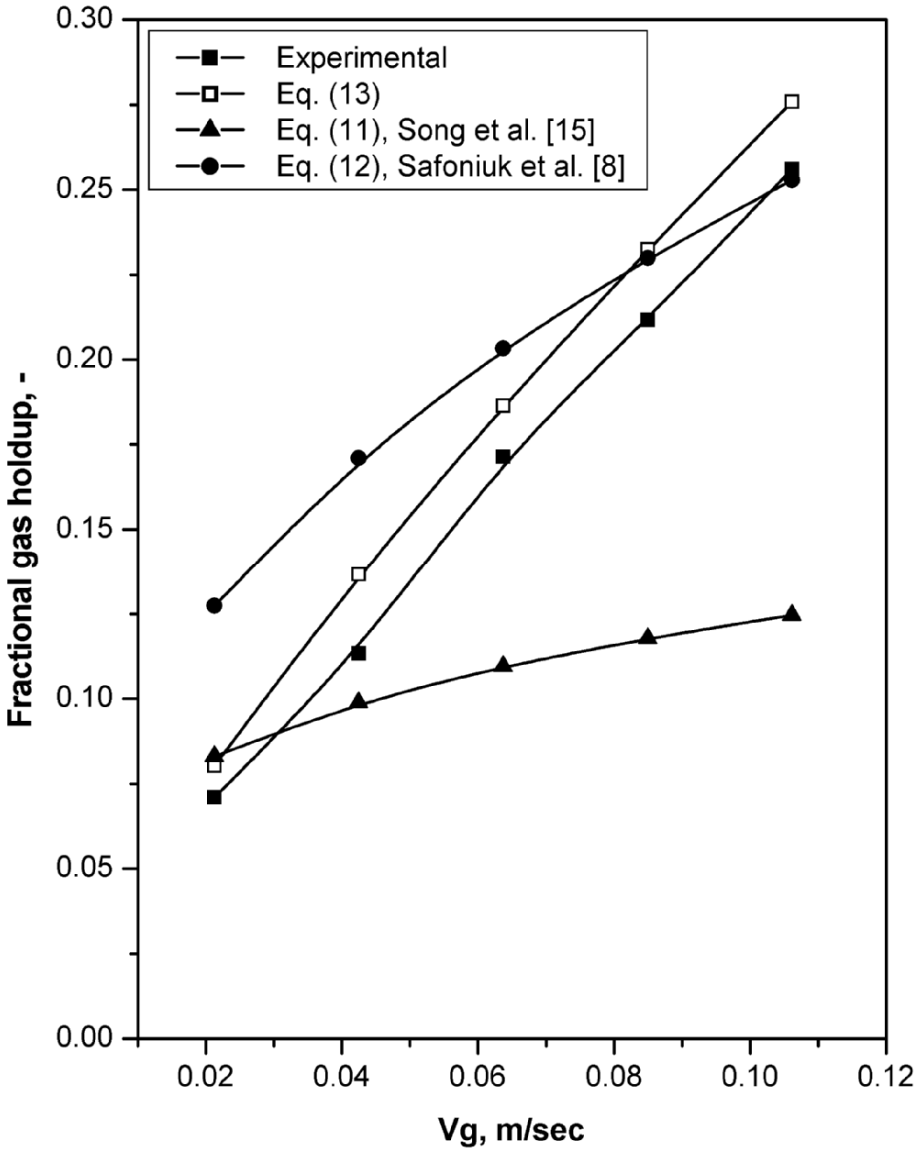

Fig. 14. Variation of gas holdup calculated from correlations and experimental with gas velocity at $H_s = 0.214$ m.

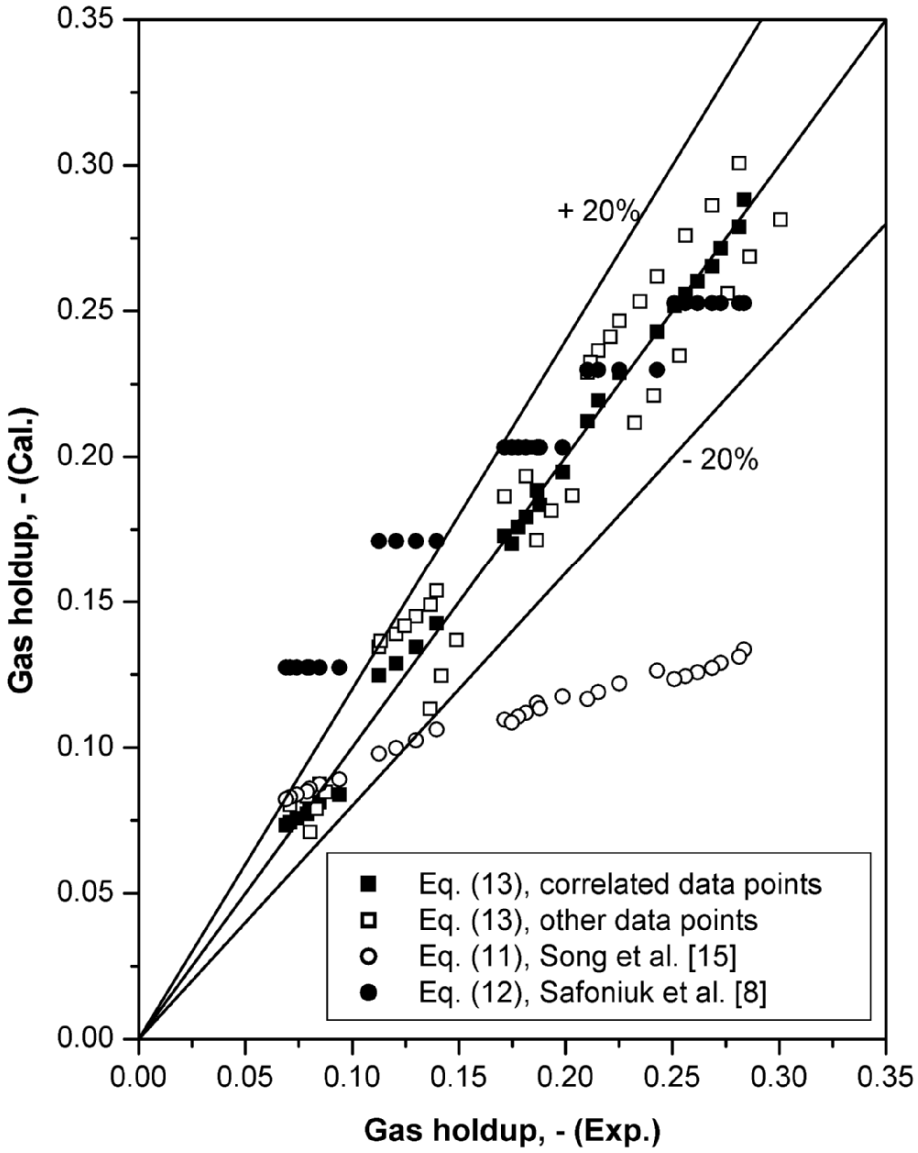

Fig. 15. Comparison of experimental values of gas hold-up with those calculated from Eqs. (9), (10) and (11).